CONFIDENCE HILLS MINERALOGY AND CHEMIN RESULTS FROM BASE OF MT. SHARP, PAHRUMP HILLS, GALE CRATER, MARS. P.D. Cavanagh[1], D.L. Bish[1], D.F. Blake[2], D.T. Vaniman[3], R.V. Morris[4], D.W. Ming[4], E.B. Rampe[4], C.N. Achilles[1], S.J. Chipera[5], A.H. Treiman[6], R.T. Downs[7], S.M. Morrison[7], K.V. Fendrich[7], A.S. Yen[8], J. Grotzinger[9], J.A. Crisp[8], T.F. Bristow[2], P.C. Sarrazin[10], J.D. Farmer[11], D.J. Des Marais[2], E.M. Stolper[9], J.M. Morookian[8], M.A. Wilson[2], N. Spanovich[8], R.C. Anderson[8] and the MSL Science Team. [1]Indiana University (pdcavana@indiana.edu), [2]NASA Ames Research Center, [3]PSI, [4]NASA Johnson Space Center, [5]CHK Energy, [6]LPI, [7]Univ. of Arizona, [8]JPL/Caltech, [9]Caltech., [10]in Xitu, Inc., [11]Arizona State Univ.

Introduction: The Mars Science Laboratory (MSL) rover *Curiosity* recently completed its fourth drill sampling of sediments on Mars. The Confidence Hills (CH) sample was drilled from a rock located in the Pahrump Hills region at the base of Mt. Sharp in Gale Crater. The CheMin X-ray diffractometer completed five nights of analysis on the sample, more than previously executed for a drill sample, and the data have been analyzed using Rietveld refinement and full-pattern fitting to determine quantitative mineralogy. Confidence Hills mineralogy has several important characteristics: 1) abundant hematite and lesser magnetite; 2) a 10 Å phyllosilicate; 3) multiple feldspars including plagioclase and alkali feldspar; 4) mafic silicates including forsterite, orthopyroxene, and two types of clinopyroxene (Ca-rich and Ca-poor), consistent with a basaltic source; and 5) minor contributions from sulfur-bearing species including jarosite.

CheMin X-ray Diffraction: The CH XRD data were processed to generate a conventional 1-D XRD pattern for analysis. Prior to conversion, instrumental artifacts (bright spots on the CCD) were removed from the image. The 1-D XRD pattern were used for phase identification, quantitative phase analysis, and background modeling . Rietveld refinement using Topas® [1] (Fig. 1) was used to determine the abundances presented in Table 1 and to refine unit-cell parameters of major and minor phases.

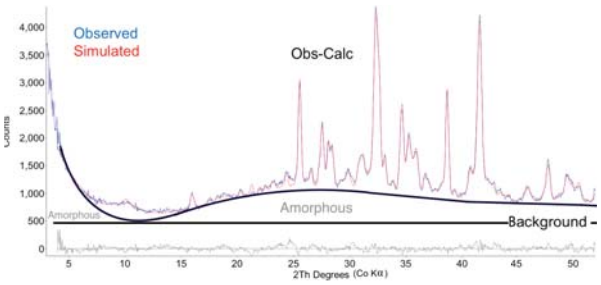

Fig. 1. CheMin Confidence Hills Rietveld refinement; simulated pattern (red) with modeled background and observed pattern (blue). The baseline shown is a modeled fit that underestimates intensities between 5 and 15, 2-theta.

Instrument Modeling. Before Rietveld refinement, information on instrumental peak shapes was obtained using data for a beryl:quartz standard measured on Mars. In addition, contributions from the Mylar sample holder and the Al light-shield were explicitly included and refined independently.

Analysis and Operations: In contrast to other sample analyses performed with CheMin, the CH sample was analyzed over five nights during sols 765, 771, 776, 778 and 785, for a total of ~37.5 hours of integration time. The additional analysis time provided improved detection of some of the minor phases including jarosite, magnetite, and pyroxene. Additionally, the integration time improved the detection of the broad and weak 10 Å phyllosilicate peak.

Mineralogy: The mineralogy of Confidence Hills (Table 1) is dominated by plagioclase, augite and hematite. Other phases present well above detection limits include a 10 Å phyllosilicate, alkali feldspar, an orthopyroxene, pigeonite, magnetite, and forsterite, as well as a significant amorphous component. Minor to trace phases close to detection limits include cristobalite, ilmenite, jarosite, and quartz. The cristobalite identification is tentative, due to significant interference of the primary diffraction peak with an Al light-shield artifact at 25.6° 2θ [2]. The suite of minerals analyzed by CheMin, including hematite, phyllosilicates, and sulfates, closely resembles the mineralogy predicted for the Murray formation by orbital observation [6].

Hematite. Hematite was identified based on large intensity for the strongest diagnostic peaks at 28.1°, 38.7°, and 41.6° 2θ. The identification of hematite by XRD also supports the latest interpretation of ChemCam spectroscopy indicating cystalline hematite [3]. The hematite abundance (~8 wt%) is significantly more than observed in other samples from Gale Crater: 0.8, 0.6, 0.7, and 0.6 wt% for Rocknest, John Klein, Cumberland, and Windjana, respectively [4,5]. The high abundance of hematite corroborates the orbital detection of hematite by VNIR spectroscopy and suggests a trend of increasing hematite abundance as Curiosity approaches the lower strata of Mount Sharp [6,7].

Clay Mineralogy. The CH XRD pattern exhibited a small broad peak at ~10 Å. Compared with the previous samples containing phyllosilicates (Fig. 2), John Klein and Cumberland, the 10 Å peak is not as well

resolved and the 02ℓ diffraction band is overlapped and obscured by pyroxene peaks and so cannot be used to distinguish among the varieties of smectite [4,5]. Based on this information, it can only be concluded that the 10 Å peak is representative of a collapsed smectite or other poorly ordered 10 Å mineral (e.g., illite), similar to that seen in John Klein. Based on results from a FULLPAT [8] analysis of the CH sample, there is ~ 11 wt% phyllosilicate.

Table 1. Confidence Hills Mineralogy – Total and crystalline phase abundance (amorphous and phyllosilicate free)

Mineral	***Abundance (wt. %)***	***Crystalline (wt. %)***
Plagioclase	22.2	37.9
Augite	7.0	12.0
Hematite	7.8	13.4
K-spar	5.7	9.7
Orthopyroxene	4.4	7.5
Pigeonite	3.8	6.5
Magnetite	2.5	4.3
Forsterite	1.9	3.3
Cristobalite	1.7*	3.0*
Ilmenite	0.9*	1.6*
Jarosite	0.2*	0.4*
Quartz	0.4*	0.6*
Phyllosilicate	11	-
Amorphous	31	-

* - At or near detection limits

Feldspars. There is evidence for multiple feldspar phases in CH. Plagioclase is the most abundant (~23 wt%) and was best modeled by two different plagioclase members, andesine (~21 wt%) and oligoclase (~2 wt%). Refined unit-cell parameters are broadly consistent with these compositions. In addition to plagioclase, K- feldspar was also detected and was best modeled using an orthoclase structure model. Overall, the feldspar mineralogy differs from Windjana (i.e., less rich in K- feldspar) and is more similar to John Klein and Cumberland. This could indicate a less-evolved mineralogy and more mafic igneous origin for the CH feldspars.

Minor Phases. The minor phases identified include: jarosite, quartz, cristobalite, and ilmenite. Although near detection limits, the jarosite identification provided a convincing improvement in fit in Rietveld refinement, particularly for the diffraction peak at ~34º 2θ. In addition, an Fe-sulfate is consistent with the SAM results of SO_2 evolution from thermal decomposition at ~600° C. As previously mentioned, the cristobalite identification is tentative because of the overlapping Al light-shield peak at 25.6° 2θ.

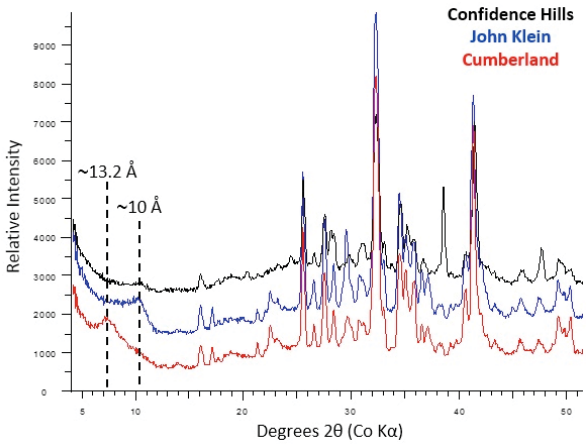

Fig. 2. Comparison of low-angle phyllosilicate peaks between Cumberland, John Klein, and Confidence Hills.

Amorphous and Phyllosilicate. As with previous samples analyzed by MSL, CH contains a large percentage of amorphous component(s). Using FULLPAT [7], it is estimated that as much as 31 wt% of the sample consists of amorphous material. If this is combined with the clay percentage, the total phyllosilicate and amorphous component of CH accounts for ~40 wt% of the sample.

Conclusions: The detection of abundant hematite, a phase rare in previous sediment samples, is consistent with the predicted suite of minerals identified from orbital spectroscopy. Spectral mapping of the Murray formation indicates a mineralogy containing a mixture of hematite, phyllosilicates, and sulfates. The CH mineralogy is consistent with the Murray formation orbital mineralogy and indicates that MSL has reached the lower strata of Mt. Sharp. The presence of hematite and iron-sulfate could also indicate that CH formed under a more acidic environment with iron-bearing fluid interaction. The CH sample also exhibits a transition to a higher abundance of plagioclase compared with the more alkali-rich previously analyzed Windjana sample. As CH represents a more basaltic mineralogy, this could indicate a different provenance and less-evolved igneous origin than Windjana.

References: [1] Bruker AXS, Karlsruhe, Germany, (2000). [2] Bish D. L. et al. (2013) Science 341, 1238932. [3] J. R. Johnson et al. *LPS XLVI*. [4] Vaniman D. T. et al. (2014) Science 343, 1243480. [5] Treiman A. H. (2015) *LPS XLVI*. [6] Milliken R. et al. (2010) Geophys. Res. Lett., 37, L04201. [7] Fraeman A. A. et al. (2013) Geology, 41(10):1103. [8] Chipera S. J. & Bish D. L. (2002) J. Appl. Crystallogr. 35, 744–749.